

Random walk on the Poincaré disk induced by a group of Möbius transformations

Charles McCarthy^{*} Gavin Nop[†]
 Reza Rastegar[‡] Alexander Roitershtein[§]

April 20, 2018; Revised: October 21, 2018

Abstract

We consider a discrete-time random motion, Markov chain on the Poincaré disk. In the basic variant of the model a particle moves along certain circular arcs within the disk, its location is determined by a composition of random Möbius transformations. We exploit an isomorphism between the underlying group of Möbius transformations and \mathbb{R} to study the random motion through its relation to a one-dimensional random walk. More specifically, we show that key geometric characteristics of the random motion, such as Busemann functions and bipolar coordinates evaluated at its location, and hyperbolic distance from the origin, can be either explicitly computed or approximated in terms of the random walk. We also consider a variant of the model where the motion is not confined to a single arc, but rather the particle switches between arcs of a parabolic pencil of circles at random times.

MSC2000: Primary: 60J05, 51M10; Secondary: 60F15, 60F10.

Keywords: random motion, random walks, Poincaré disk, random Möbius transformations, iterated random functions, gyrotranslations, bipolar coordinates, limit theorems.

1 Introduction

The aim of this paper is to introduce a certain random motion on the Poincaré disk and study its basic asymptotic properties. This motion is induced by an iterated random functions (IRF) model, where the functions are Möbius transformations drawn at random from the family introduced in Section 2. The majority of our work is thus the study of this specific family of Möbius transformations and their associated IRF model. The primary feature of

^{*}Department of Mathematics, Iowa State University, Ames, IA 50011, USA; e-mail: lasker@iastate.edu

[†]Department of Mathematics, Iowa State University, Ames, IA 50011, USA; e-mail: gnnop@iastate.edu

[‡]Occidental Petroleum Corporation, Houston, TX 77046 and Departments of Mathematics and Engineering, University of Tulsa, OK 74104, USA - Adjunct Professor; e-mail: reza_rastegar2@oxy.com

[§]Department of Statistics, Texas A&M University, College Station, TX 77843, USA; e-mail: alexander@stat.tamu.edu

our focus is the convergence of iterations. Conditions for the convergence of a sequence of compositions of Möbius transformations are well-known [1, 19]. A standard condition implies that almost every member in the underlying family of transformations should have a common attractive fixed point. In fact, under mild technical assumption this condition is necessary and sufficient for an IRF model to converge. The underlying family of Möbius transformations considered in this paper can be characterized by the assumption that all the transformations are one-to-one on the unit disk and have two common fixed points along with a natural maximality property (see Section 2, in particular Proposition 2.1).

It turns out that after a proper re-parametrization and using some intrinsic coordinates, various features of our studied IRF can be quantified in terms of a one-dimensional random walk. The relation between the induced motion in the Poincaré disk and the random walk on \mathbb{R} is the key tool we use to study the former. The random motion can be seen as a mixture of basic IRFs in a fashion similar to the way a random walk on \mathbb{Z}^2 can be perceived as a mixture of random walks on \mathbb{Z} . Furthermore, an orbit of each of the basic IRF model is contained within an arc in the unit disk connecting two opposite points on the perimeter of the unit disk which are common fixed points of the underlying Möbius transformations (dotted horizontal lines in Fig. 1 below). The vertical arcs are geodesic lines in the Poincaré disk model whereas the horizontal are not. In the second part of the paper we consider a genuinely two-dimensional walk on the Poincaré disk where (similarly to the classical simple random walk on \mathbb{Z}^2) at each jump the random walk moves along either dotted or dashed circles and thus preserves one of the two intrinsic coordinates, current direction being decided by a regular coin-tossing procedure. Remark that typically, a discrete-time random walk on a hyperbolic space [13, 22, 25] or, more generally, on a Riemannian manifold [18, 26] is a motion along geodesic lines.

The paper is structured as follows. In Section 2 we introduce a family (an abelian subgroup) of Möbius transformations that governs the “horizontal” portion of the random motion. In Sections 3 and 4 we consider the basic IRF that represents the horizontal part of the random motion in our model. The functions in the IRF model are Möbius transformations drawn at random from the family introduced in Section 2. To study the IRF we introduce in Section 3 so-called bipolar coordinates whose isoparametric curves are represented by two orthogonal sets (pencils) of circular arcs (see Fig. 1). In Section 3 we compute certain geometric characteristics of the auxiliary IRF process, and in Section 4 we discuss the rate of its attraction to the disk boundary in various regimes. In Section 5 we apply these results to study a genuinely two-dimensional motion on \mathcal{D} that is in some natural fashion induced by the above auxiliary process. These are the main results of this paper and are concerned with the asymptotic behavior of the random motion. Finally, in Section 6 we present some numerical simulations for the motion introduced in Section 5.

2 An abelian group of Möbius transformations

In this section we introduce a family of Möbius transformations that govern the “horizontal” (i. e., along dashed arcs in Fig. 1 above) motion in our model.

Let \mathcal{D} be open unit disk with center at 0 in the complex plane \mathbb{C} . Recall that the Poincaré

distance $d_{\mathfrak{p}}(z, w)$ between two points $z, w \in \mathcal{D}$ is given by

$$d_{\mathfrak{p}}(z, w) = \log \left(\frac{1 + \rho_{z,w}}{1 - \rho_{z,w}} \right) = \operatorname{arctanh} \rho_{z,w}, \quad \text{where } \rho_{z,w} := \left| \frac{z - w}{1 - \bar{z}w} \right|. \quad (1)$$

The choice of the constant in front of the logarithm is a matter of convention, it is often set to be $\frac{1}{2}$. The Poincaré disk $(\mathcal{D}, d_{\mathfrak{p}})$ is a canonical model of the hyperbolic space. Let $\overline{\mathcal{D}}$ be the closure of \mathcal{D} in \mathbb{C} and $\partial\mathcal{D}$ be its boundary, a unit circle. Let $\alpha \in \partial\mathcal{D}$ be given, it will remain fixed throughout the paper.

We will be concerned with Möbius transformations $q_{x,\alpha} : \overline{\mathcal{D}} \rightarrow \overline{\mathcal{D}}$ defined for $\alpha \in \partial\mathcal{D}$ and real $x \in (-1, 1)$ by

$$q_{x,\alpha}(z) = \frac{z + x\alpha}{1 + x\bar{\alpha}z}, \quad z \in \overline{\mathcal{D}}. \quad (2)$$

In the language of [32, 33], the kind of Möbius transformations that appears in (2) (namely, $z \oplus w := \frac{z+w}{1+\bar{w}z}$ with $w = x\alpha$) is called a gyrotranslation. This particular class of Möbius transformations plays a fundamental role in hyperbolic geometry and its applications (for instance, notice that $\rho_{z,w}$ in (1) is $|z \oplus (-w)|$).

Remark that for any $\alpha \in \partial\mathcal{D}$ and $x \in (-1, 0) \cup (0, 1)$,

- (i) $q_{x,\alpha}$ is a holomorphic automorphism (one-to-one and onto map) of \mathcal{D} .
- (ii) $q_{x,\alpha}$ stabilizes the boundary $\partial\mathcal{D}$. That is, $q_{x,\alpha}(\partial\mathcal{D}) = \partial\mathcal{D}$.
- (iii) $q_{x,\alpha}$ has two fixed points, $-\alpha$ and α . That is, $q_{x,\alpha}(-\alpha) = -\alpha$ and $q_{x,\alpha}(\alpha) = \alpha$.

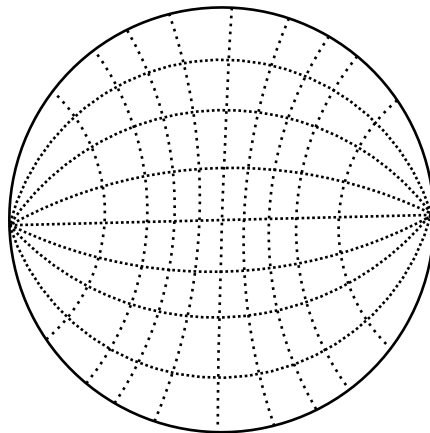


Figure 1: Two orthogonal pencils of coaxial circles. Dashed circles are centered on the y axis and go through the points -1 and 1 . Dotted circles are centered on the x axis and intersect dashed circles at the right angle.

In fact, any transformation of \mathcal{D} that has property (i) is in the form $\beta q_{x,\alpha}$ for some $\alpha, \beta \in \partial\mathcal{D}$, and hence posses property (ii) as well. Let $Q_\alpha := \{q_{x,\alpha} : x \in (-1, 1)\}$. Note that Q_α is closed under finite compositions of its elements. More precisely, for any $x_1, x_2 \in (-1, 1)$, there is a unique $x \in (-1, 1)$ such that

$$q_{x_1,\alpha} \circ q_{x_2,\alpha} = q_{x,\alpha}, \quad \text{where } \frac{1+x}{1-x} = \frac{1+x_1}{1-x_1} \cdot \frac{1+x_2}{1-x_2}. \quad (3)$$

Our results in the next sections rely on the asymptotic properties of iterated compositions of random elements of Q_α . Property (iii) which guarantees that all transformations in the family Q_α have a common fixed point is the main reason why we exclude the composition with a rotation from our consideration. It is well-known that a sequence of iterated Möbius transformation necessarily diverges unless all the transformations have a common fixed point w.p.1 (with probability one) [1, 19]. The feature of Q_α 's that originally spiked our interest in these collections of Möbius transformations can be described as follows:

Proposition 2.1. *Q_α for $\alpha \in \partial\mathcal{D}$ is a maximal family of transformations on $\overline{\mathcal{D}}$ such that its elements are holomorphic bijections on \mathcal{D} , all having two common fixed points. Conversely, any such maximal family is either Q_α for some $\alpha \in \partial\mathcal{D}$ or consists of exactly one element.*

Proof. Any holomorphic bijections on \mathcal{D} has the form $f(z) = \beta q_{x,\alpha} = \beta \frac{z+x\alpha}{1+x\bar{\alpha}z}$ for some $\alpha, \beta \in \partial\mathcal{D}$ and $x \in (-1, 1)$. Our goal is to show that either $\beta = 1$ or there is no other holomorphic bijections on \mathcal{D} having the same two fixed point as f . Let $z = \alpha\omega$ be a non-zero fixed point of f . Then

$$\omega = \beta \frac{\omega + x}{1 + x\bar{\omega}}. \quad (4)$$

Since $|\beta| = 1$ this implies that $|\omega + x| |\omega|^2 = |\omega + x|$. It is easy to see that this identity is only possible if either $|\omega| = 1$ or $x = 0$ or $x = -\frac{2\operatorname{Re}(\omega)}{1+|\omega|^2}$. If $x = 0$ then $\beta = 1$ and hence $f \in Q_\alpha$. If $|\omega| = 1$ then (4) yields $\omega + x = \beta(\omega + x)$ and thus $\beta = 1$ and $f \in Q_\alpha$. Finally, if $x = -\frac{2\operatorname{Re}(\omega)}{1+|\omega|^2}$ and $|\omega| \neq 1$ then x and due to (4) also β are uniquely determined by ω , implying that f is a unique holomorphic bijections on \mathcal{D} having $z = \alpha\omega$ as its fixed point. \square

In view of (3), the family of transformations Q_α is more conveniently parametrized using the parameter

$$\gamma(x) = \log\left(\frac{1+x}{1-x}\right) = \operatorname{sign}(x) \cdot d_{\mathbf{p}}(0, x\alpha) \quad (5)$$

rather than x (see (8) below). Note that $\gamma : (-1, 1) \rightarrow \mathbb{R}$ is a one-to-one transformation. In addition to the representation as the right-most expression in (5), another illuminating interpretation of $\gamma(x)$ is that

$$e^{\gamma(x)} = \frac{1+x}{1-x} = \frac{d}{dz} q_{x,\alpha}(-\alpha) = \left(\frac{d}{dz} q_{x,\alpha}(\alpha) \right)^{-1}. \quad (6)$$

In what follows, for a given $\alpha \in \partial\mathcal{D}$, we denote

$$g_\gamma := q_{x,\alpha} \quad \text{if} \quad \gamma = \log\left(\frac{1+x}{1-x}\right). \quad (7)$$

In this notation (3) reads

$$g_{\gamma_1} \circ g_{\gamma_2} = g_{\gamma_2} \circ g_{\gamma_1} = g_{\gamma_1 + \gamma_2}. \quad (8)$$

Thus

$$G_\alpha := \{g_\gamma : \gamma \in \mathbb{R}\} \quad (9)$$

form an abelian group of transformations on $\overline{\mathcal{D}}$.

Let $x = (x_n)_{n \in \mathbb{N}}$ be a stationary and ergodic sequence of random variables valued in the interval $(-1, 1)$. Specific assumptions on the distribution of x will be made in Section 4. Let

$$\rho_n = \frac{1 + x_n}{1 - x_n} \quad \text{and} \quad \gamma_n = \log \rho_n.$$

Consider a (generalized) random walk on \mathbb{R} defined by the partial sums of the sequence γ_n :

$$\omega_0 := 0 \quad \text{and} \quad \omega_n := \sum_{i=1}^n \gamma_i, \quad n \in \mathbb{N}. \quad (10)$$

For a comprehensive treatment of regular random walks on \mathbb{R} (partial sums of i. i. d. random variables) see, for instance, monographs [9, 28]. For recent results and literature survey on partial sums of dependent real-valued variables see, for instance, [4, 17, 31].

The random walk ω_n induces a random walk on the elements of the group G_α :

$$U_n := g_{\omega_n}, \quad n \in \mathbb{Z}_+.$$

Here and thereafter, \mathbb{Z}_+ stands for the set of non-negative integers $\mathbb{N} \cup \{0\}$.

It follows from (8) that for any permutation $\sigma : \{1, 2, \dots, n\} \rightarrow \{1, 2, \dots, n\}$,

$$U_n = g_{\gamma_{\sigma(1)}} \circ g_{\gamma_{\sigma(2)}} \circ \dots \circ g_{\gamma_{\sigma(n)}}, \quad (11)$$

and

$$U_n(z) = \frac{z + y_n \alpha}{1 + y_n \bar{\alpha} z}, \quad (12)$$

with $y_n \in (-1, 1)$ such that

$$\frac{1 + y_n}{1 - y_n} = \prod_{k=1}^n \rho_k = e^{\omega_n}. \quad (13)$$

In view of (6) and (11), the identity (13) can be thought as a direct implication of the chain rule formula $U'_n(\alpha) = g'_{\gamma_n}(\alpha) \cdot U'_{n-1}(\alpha)$.

We observe in Lemma 3.1 below that the entire orbit $\{U_n(z) : n \in \mathbb{N}\}$ lies on the circular arc going through the poles $-\alpha, \alpha$, and the initial position $z \in \overline{\mathcal{D}}$.

3 Locus of the orbits $\{U_n(z)\}_{n \in \mathbb{N}}$ in the hyperbolic disk

The goal of this section is to explicitly relate certain geometric characteristics of $U_n(z)$ to the random walk ω_n . The relation can be subsequently exploited in order to deduce the asymptotic behavior of $U_n(z)$ from standard limit theorems for ω_n .

The main results of this section are Lemma 3.1 asserting that the orbit $(U_n(z))_{n \in \mathbb{Z}_+}$ belongs to a circle which is invariant under the transformations of group G_α , Lemma 3.7 that can serve, for instance, to calculate the rate of convergence of a transient process U_n to the boundary (see Theorem 4.2 in Section 4), and Lemma 3.4 that establishes the location of $U_n(z)$ in terms of certain, intrinsic to the problem, bipolar coordinates (for an example of application see Proposition 4.9 in Section 4).

Let \bar{l}_α and l_α denote, respectively, the diameter of \mathcal{D} connecting α and $-\alpha$ and its interior. That is,

$$l_\alpha = \{z \in \mathcal{D} : z = x\alpha \text{ for some } x \in (-1, 1)\} \quad \text{and} \quad \bar{l}_\alpha = l_\alpha \cup \{-\alpha, \alpha\}. \quad (14)$$

Note that \bar{l}_α is invariant under U_n for all $n \in \mathbb{Z}$. In fact,

$$U_n(x\alpha) = \alpha \frac{x + y_n}{1 + xy_n}, \quad x \in [-1, 1]. \quad (15)$$

In the general case we have the following lemma:

Lemma 3.1. *For an arbitrary $z \in \bar{\mathcal{D}} \setminus \{-\alpha, \alpha\}$, the orbit $\{U_n(z)\}_{n \in \mathbb{N}}$ lies entirely on the circle H_z through the three points $\alpha, -\alpha$, and z .*

Remark 3.2. *If $z \in l_\alpha$, then the circle H_z is degenerate according to (15). Namely, it is the straight line that contains the segment l_α .*

Proof of Lemma 3.1. For $z \in l_\alpha$ the result follows directly from (15). For $z \in \bar{\mathcal{D}} \setminus \bar{l}_\alpha$, letting $u_n = y_n\alpha$, we get $U_n(z) = \alpha^2 \frac{z + u_n}{\alpha^2 + zu_n}$. Thus for a fixed $z \in \bar{\mathcal{D}} \setminus \bar{l}_\alpha$, the orbit $\{U_n(z)\}_{n \in \mathbb{Z}_+}$ lies entirely within the image of l_α under the Möbius transformation

$$T_z(u) := \alpha^2 \frac{z + u}{\alpha^2 + zu}. \quad (16)$$

The image of a line under a Möbius transformation is either a line or a circle. The result then follows from the observation that $T_z(-\alpha) = -\alpha$, $T_z(\alpha) = \alpha$, and $T_z(0) = z$. \square

Remark 3.3.

(i) *The proof of Lemma 3.1 which is given above suggests the following parametrization of the arc $H_z \cap \mathcal{D}$. Recall that the arc is the image of the diameter l_α under the transformation T_z . Thus it is natural to parametrize it by associating a point $w \in H_z \cap \mathcal{D}$ with the real parameter $\bar{\alpha}T_z^{-1}(w)$, or perhaps with $\gamma(\bar{\alpha}T_z^{-1}(w))$, where $\gamma : (-1, 1) \rightarrow \mathbb{R}$ is defined in (5). The former variation is essentially (up to a constant) the chord-length parametrization of the arc $H_z \cap \mathcal{D}$ in the language of [29]. For the sake of technical convenience, we choose the latter variant. More specifically, define $\hat{\tau}_z : \mathbb{R} \rightarrow H_z \cap \mathcal{D}$ by*

$$\hat{\tau}_z(\delta) = T_z(\gamma^{-1}(\delta) \cdot \alpha). \quad (17)$$

Notice that due to the isometry property of Möbius transformations, for any

$$\delta_1 = \gamma(x_1) = \log\left(\frac{1+x_1}{1-x_1}\right) \quad \text{and} \quad \delta_2 = \gamma(x_2) = \log\left(\frac{1+x_2}{1-x_2}\right), \quad x_1, x_2 \in (-1, 1),$$

we have

$$d_{\mathfrak{p}}(\hat{\tau}_z(\delta_1), \hat{\tau}_z(\delta_2)) = d_{\mathfrak{p}}(x_1\alpha, x_2\alpha) = d_{\mathfrak{p}}(x_1, x_2) = |\gamma(x_1) - \gamma(x_2)|.$$

A slight modification of the parametrization $\hat{\tau}_z$ introduced in (17) plays a central role in our study (cf. (21), Remark 3.5 and Lemma 3.4 below). Note that by virtue of (12) and (13), the definition (17) implies that

$$U_n(z) = \hat{\tau}_z(\omega_n). \quad (18)$$

(ii) An alternative short proof of the lemma follows from the parametric definition of the circle H_z given in (19) below and (20) which identifies the (hyperbolic, e. g. having two distinct fixed points) Möbius transformation $U_z(z)$ in terms of its fixed points and derivatives at those points (see, for instance, [21, p. 22]).

For a given initial point $z \in \overline{\mathcal{D}} \setminus \{-\alpha, \alpha\}$, an equation of the circle in Lemma 3.1 can be written as

$$H_z = \left\{ u \in \mathbb{C} : \frac{u+\alpha}{u-\alpha} \cdot \frac{z-\alpha}{z+\alpha} \in \mathbb{R} \right\}. \quad (19)$$

Note that for $z \in l_\alpha$, the circle H_z is degenerate, namely H_z is the straight line which contains the segment l_α . A direct computation exploiting (12) shows that for $u = U_n(z)$ in (19) we have

$$\frac{U_n(z) + \alpha}{U_n(z) - \alpha} = \frac{z + \alpha}{z - \alpha} \cdot \frac{1 + y_n}{1 - y_n} = \frac{z + \alpha}{z - \alpha} \cdot e^{\omega_n}, \quad z \in \overline{\mathcal{D}} \setminus \{-\alpha, \alpha\}. \quad (20)$$

Writing $\frac{1+y_n}{1-y_n}$ as $\frac{\alpha+y_n\alpha}{\alpha-y_n\alpha}$, the last formula can be seen as a direct implication of the following instance of the cross-ratio property of the Möbius transformation U_n :

$$\frac{U_n(z) - U_n(-\alpha)}{U_n(z) - U_n(\alpha)} \cdot \frac{U_n(0) - U_n(\alpha)}{U_n(0) - U_n(-\alpha)} = \frac{z - (-\alpha)}{z - \alpha} \cdot \frac{0 - \alpha}{0 - (-\alpha)}.$$

It is not hard to verify that the center of the circle H_z is at the point $-i\alpha c$ and its radius is $\sqrt{1+c^2}$, where c is the unique solution to $|z + i\alpha c|^2 = 1 + c^2$, that is $c = \frac{1-|z|^2}{2i(\bar{z}\alpha - z\bar{\alpha})}$. These explicit formulas are not used anywhere in the sequel and are given here for the sake of completeness only.

We next consider *bipolar coordinates* [6, 16, 29] associated with the pair $(\alpha, -\alpha)$. For $z \in \mathbb{C}$ we let

$$\tau(z) = \log \frac{|z + \alpha|}{|z - \alpha|} \quad \text{and} \quad \sigma(z) = \text{sign}(\text{Im}(\bar{\alpha}z)) \cdot \angle(-\alpha, z, \alpha), \quad (21)$$

where $\angle(A, B, C) \in (0, \pi]$ is the angle B in the triangle formed by the vertexes A, B , and C in the complex plane. Thus $\tau(z) \in (0, \infty)$, $\sigma(z) = \pi$ if $z \in l_\alpha$, $\sigma(z) > 0$ if the orientation of

the circular arc going from α to $-\alpha$ through z is anticlockwise, $\sigma(z) < 0$ otherwise, and we convene that $\sigma \in (\frac{\pi}{2}, \pi] \cup (-\pi, -\frac{\pi}{2})$ for $z \in \mathcal{D}$ (see Fig. 2 below).

It can be shown that [16]

$$z = \alpha i \cot\left(\frac{\sigma(z) + i\tau(z)}{2}\right). \quad (22)$$

In a somewhat more explicit form, if $z = x + iy$, then assuming for simplicity $\alpha = 1$, one obtains [6, 16, 29]

$$x = \frac{\sinh \tau(z)}{\cosh \tau(z) - \cos \sigma(z)} \quad \text{and} \quad y = \frac{\sin \sigma(z)}{\cosh \tau(z) - \cos \sigma(z)}. \quad (23)$$

The bipolar coordinates are commonly used to separate variables in equations of mathematical physics when the Laplace operator is the dominated term (the idea goes back to [5], see, for instance, [8, 10, 16, 24]).

Lemma 3.1 and (20) together imply the following:

Lemma 3.4. *For any $n \in \mathbb{Z}_+$ and $z \in \mathcal{D} \setminus \{-\alpha, \alpha\}$ we have*

$$\tau(U_n(z)) = \tau(z) + \omega_n \quad \text{and} \quad \sigma(U_n(z)) = \sigma(z).$$

Thus the displacement of the τ -coordinate $\tau(U_n(z))$ relatively to the initial value $\tau(z)$ is equivalent to a partial sum of suitable i. i. d. variables.

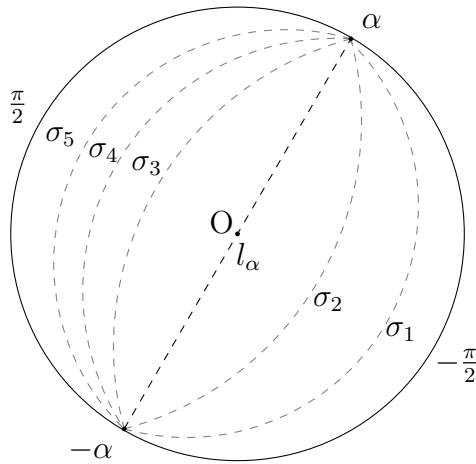


Figure 2: The circles H_z are isoparametric curves for the bipolar coordinate σ , that is the value of σ is constant on each circle. For σ 's associated with the dashed circles in the picture, we have $-\pi < \sigma_2 < \sigma_1 < -\frac{\pi}{2}$ and $\frac{\pi}{2} < \sigma_5 < \sigma_4 < \sigma_3 < \pi$. Furthermore, $\sigma(z) = \pm\frac{\pi}{2}$ for $z \in \partial\mathcal{D}$ and $\sigma(z) = \pi$ for $z \in \bar{l}_\alpha$. The location of a point z on a dashed circle can be determined using the second coordinate τ , which is the logarithm of the ratio of the Euclidean distances from z to $-\alpha$ and from z to α . It can be shown that τ is constant on arcs orthogonal to the dashed ones (see Fig. 1 above).

Remark 3.5. A comparison Lemma 3.4 with (18) indicates that the function $\tau(u)$ is a shifted version of the inverse of $\hat{\tau}_z(u)$ introduced in (17) for any $z \in \mathcal{D}$. Indeed, it is not hard to verify that in general

$$\tau(g_\gamma(z)) = \tau(z) + \gamma = \tau(z) + \hat{\tau}_z^{-1}(g_\gamma(z)), \quad \forall \gamma \in \mathbb{R}, z \in \mathcal{D},$$

where g_γ is the Möbius transformation defined in (7).

The following result (cf. formula (8) in [20]) is equivalent to the particular case of Lemma 3.4 when $|z| = 1$.

Corollary 3.6. For $n \in \mathbb{Z}_+$ and $z \in \partial\mathcal{D} \setminus \{-\alpha, \alpha\}$, let

$$\psi_n^-(z) := \angle(U_n(z), 0, \alpha) \quad \text{and} \quad \psi_n^+(z) := \angle(U_n(z), 0, -\alpha).$$

Then, for all $n \in \mathbb{Z}_+$ and $z \in \partial\mathcal{D} \setminus \{-\alpha, \alpha\}$,

$$\tan\left(\frac{\psi_n^+(z)}{2}\right) = e^{\omega_n} \cdot \tan\left(\frac{\psi_0^+(z)}{2}\right),$$

and, correspondingly,

$$\tan\left(\frac{\psi_n^-(z)}{2}\right) = e^{-\omega_n} \cdot \tan\left(\frac{\psi_0^-(z)}{2}\right).$$

Proof. Proof of Corollary 3.6 Note that for $z \in \partial\mathcal{D} \setminus l_\alpha$,

$$\frac{\psi_n^-}{2} = \angle(U_n(z), -\alpha, \alpha) \quad \text{and} \quad \frac{\psi_n^+}{2} = \angle(U_n(z), \alpha, -\alpha). \quad (24)$$

Thus for $z \in \partial\mathcal{D}$, we have

$$\tau(U_n(z)) = \log\left(\tan \frac{\psi_n^+}{2}\right),$$

and hence the result in Corollary 3.6 is a direct implication of Lemma 3.4. \square

Recall that in the Poincaré disc model, Busemann function corresponding to $\xi \in \partial\mathcal{D}$ is given by [11, 12]

$$B_\xi(z) = -\log\left(\frac{1 - |z|^2}{|\xi - z|^2}\right), \quad z \in \mathcal{D}. \quad (25)$$

Note that $B_\xi(0) = 0$, $\lim_{z \rightarrow \xi} B_\xi(z) = -\infty$, and $\lim_{z \rightarrow \zeta} B_\xi(z) = +\infty$ for any $\zeta \in \mathcal{D}$ such that $\zeta \neq \xi$. Intuitively, a Busemann function B_ξ is the distance function on \mathcal{D} from a point $\xi \in \partial\mathcal{D}$ “at infinity”. A rigorous definition utilizing this heuristics and the disc boundary $\partial\mathcal{D}$ as “the infinity” is as follows:

$$B_\xi(z) = \lim_{x \rightarrow 1^-} [d_p(z, x\xi) - d_p(0, x\xi)], \quad \xi \in \partial\mathcal{D}, z \in \mathcal{D}.$$

The function within the brackets in (25) is the Poisson kernel of the unit disk, the density of a harmonic measure on the disk's boundary [3, 15]. The interpretation of $\frac{1}{2\pi} \frac{1-|z|^2}{|e^{i\theta}-z|^2} d\theta$ as the density of the standard (Euclidean) planar Brownian motion starting at $z \in \mathcal{D}$ and evaluated at the first hitting time of $\partial\mathcal{D}$ provides a link between the Busemann functions and the theory of Brownian motion. We remark that in the context of statistical applications with circular data, the distribution on $\partial\mathcal{D}$ with this density is often referred to as a circular or wrapped Cauchy distribution [20]. The curious link between Busemann functions, the probabilistic interpretation of the Poisson kernels, and canonical iterative models of circular data in statistics is not used anywhere in the sequel and is brought here for the sake of completeness only.

From (13) we obtain the following expression for y_n :

$$y_n = \frac{e^{\omega_n} - 1}{e^{\omega_n} + 1}. \quad (26)$$

Substituting (12) and (26) into (25) yields the following:

Proposition 3.7. *For all $z \in \mathcal{D}$ and $n \in \mathbb{Z}_+$,*

$$B_\alpha(U_n(z)) = -\omega_n + B_\alpha(z) \quad \text{and} \quad B_{-\alpha}(U_n(z)) = \omega_n + B_{-\alpha}(z).$$

This observation allows us to immediately translate any result for the random walk ω_n into a counterpart statement about the behavior of Busemann functions $B_{\pm\alpha}(U_n(z))$. For an example of application of Proposition 3.7 see Theorem 4.2 below.

Remark 3.8. *The result in Proposition 3.7 can be also seen as a direct implication of the formula (20) because of the Poisson kernel identity $\frac{1-|z|^2}{|\xi-z|^2} = \operatorname{Re}\left(\frac{\xi+z}{\xi-z}\right)$, $\xi \in \partial\mathcal{D}$ and $z \in \mathcal{D}$.*

The following lemma complements the result in Lemma 3.1 by highlighting the choice of the direction of the motion along the circle H_z .

Lemma 3.9. *For all $n \in \mathbb{N}$, $z \in \mathcal{D} \setminus \{-\alpha, \alpha\}$ and $\varepsilon \in \{-1, 1\}$, the following statements are equivalent:*

- (i) $|U_n(z) - \varepsilon\alpha| < |U_{n-1}(z) - \varepsilon\alpha|$.
- (ii) $\varepsilon x_n > 0$.
- (iii) $\varepsilon \gamma_n > 0$.
- (iv) $B_{\varepsilon\alpha}(U_n(z)) < B_{\varepsilon\alpha}(U_{n-1}(z))$.

Proof of Lemma 3.9. The equivalence of (ii) and (iii) is trivial. The equivalence of (iii) and (iv) follows from Proposition 3.7. It remains to show the equivalence of (i) and (ii). To this end observe that the orbit $\{U_n(z)\}_{n \in \mathbb{Z}_+}$ is the image of $\{y_n\alpha\}_{n \in \mathbb{Z}_+}$ under a conformal transformation T_z , which is defined in (16). By virtue of Lemma 3.1, the claim is a consequence of the fact that T_z is preserving the orientation of curves, \square

An explicit formula for the hyperbolic distance $d_p(0, U_n(z))$ in terms of the initial bipolar coordinates $(\sigma(z), \tau(z))$ can be in principle obtained from (12) and (23). We conclude this subsection with the following approximation result.

Lemma 3.10. *For all $z \in \mathcal{D}$ and $n \in \mathbb{N}$, we have $|d_p(0, U_n(z)) - |\omega_n|| \leq d_p(0, z)$.*

Proof of Lemma 3.10. First, observe that since $0 = U_n(-y_n\alpha)$,

$$d_p(U_n(0), 0) = d_p(0, -y_n\alpha) = \log\left(\frac{1 + |y_n|}{1 - |y_n|}\right) = \left|\log\left(\frac{1 + y_n}{1 - y_n}\right)\right| = |\omega_n|,$$

where the first identity is implied by the isometry property of Möbius transformation U_n . Next, the identity $d_p(U_n(0), 0) = |\omega_n|$ can be utilized to deduce the asymptotic behavior of $d_p(U_n(z), 0)$ for an arbitrary $z \in \mathcal{D}$ through the following triangle inequalities:

$$d_p(U_n(z), 0) \leq d_p(U_n(z), U_n(0)) + d_p(U_n(0), 0) = d_p(z, 0) + d_p(U_n(0), 0) \quad (27)$$

and

$$d_p(U_n(z), 0) \geq d_p(U_n(0), 0) - d_p(U_n(0), U_n(z)) = d_p(U_n(0), 0) - d_p(z, 0), \quad (28)$$

where the equalities are due to the isometry property of Möbius transformations. \square

For an example of applications of Lemmas 3.4 and 3.10 see Proposition 4.9 below.

4 Convergence to the boundary of the disk

In this section we study the convergence of $U_n(z)$ to the disk boundary $\partial\mathcal{D}$, more precisely to the pair set $\mathcal{A} = \{-\alpha, \alpha\}$. Heuristically, $\lim_{n \rightarrow \infty} |\omega_n| = +\infty$ in probability (almost surely in a transient regime) for standard models of random walk on \mathbb{R} . Hence, in a suitable mode of convergence, \mathcal{A} is typically an attractor for U_n (for instance, by Proposition 3.7 above). The goal of this section is to characterize this convergence in terms of basic properties of the random walk ω_n .

First we impose the following basic assumption on the sequence $(x_n)_{n \in \mathbb{N}}$.

Assumption 4.1.

- (A1) $(x_n)_{n \in \mathbb{N}}$ is a stationary and ergodic sequence.
- (A2) $P(x_1 \in (-1, 1)) = 1$.
- (A3) Let $\gamma_n = \log\left(\frac{1+x_n}{1-x_n}\right)$. Then $E(\gamma_1)$ is well defined, possibly infinite.

We denote

$$\varepsilon_x = \text{sign}(E(\gamma_1)). \quad (29)$$

It follows from a general result of [19] for a composition of random Möbius transformations that if Assumption 4.1 holds and $\varepsilon_x \neq 0$ then, with probability one, for any $z \in \overline{\mathcal{D}} \setminus \{-\alpha, \alpha\}$,

$$\lim_{n \rightarrow \infty} U_n(z) = \varepsilon_x \alpha. \quad (30)$$

Formally, (30) is proved in [19] only for i.i.d. sequences x_n , but it is straightforward to see that their argument works verbatim under Assumption 4.1. The rate of escape to the boundary can be quantified using results from the previous section. Namely, by virtue of Lemma 3.4 and Proposition 3.7 we have the following:

Theorem 4.2. *Let Assumption 4.1 hold and assume in addition that $\varepsilon_x \neq 0$. Then w. p. 1,*

$$\lim_{n \rightarrow \infty} \frac{1}{n} B_{\varepsilon_x \alpha}(U_n(z)) = -|E(\gamma_1)| \quad \text{and} \quad \lim_{n \rightarrow \infty} \frac{1}{n} d_{\mathbb{P}}(0, U_n(z)) = |E(\gamma_1)|$$

for all $z \in \mathcal{D}$.

Our next result gives the rate of convergence in terms of the Euclidean distance. For $\delta > 0$ and $z \in \mathbb{C}$ let $N_\delta(z) = \{w \in \mathbb{C} : |z - w| < \delta\}$. Denote $\overline{\mathcal{D}}_\delta := \overline{\mathcal{D}} \setminus (N_\delta(\alpha) \cap N_\delta(-\alpha))$. We have:

Theorem 4.3. *Suppose that Assumption 4.1 is satisfied. If $\varepsilon_x \neq 0$, then for any $\delta > 0$, the following holds w. p. 1:*

$$\lim_{n \rightarrow \infty} \frac{1}{n} \log \left(\sup_{z \in \overline{\mathcal{D}}_\delta} |U_n(z) - \varepsilon_x \alpha| \right) = -|E(\gamma_1)|.$$

Remark 4.4. *Without the uniformity of the convergence, the result in Theorem 4.3 follows directly from (30) and (20). We give below a short self-contained proof that doesn't assume (30) a-priori and, more importantly, yields the uniformity. In addition, the calculation can be generalized readily to include other modes of convergence besides the almost sure one. See, for instance, Theorem 4.8 and Proposition 4 below.*

Proof of Theorem 4.3. For $\varepsilon \in \{-1, 1\}$ write

$$U_n(z) - \varepsilon \alpha = \frac{z + y_n \alpha - \varepsilon(\alpha + y_n z)}{1 + y_n \bar{\alpha} z} = \frac{(z - \varepsilon \alpha)(1 - \varepsilon y_n)}{1 + y_n \bar{\alpha} z}. \quad (31)$$

Birkhoff's ergodic theorem implies that

$$\lim_{n \rightarrow \infty} \omega_n = \varepsilon_x \cdot \infty, \quad \text{a. s.}$$

It follows then from (26) that

$$\lim_{n \rightarrow \infty} y_n = \varepsilon_x, \quad \text{a. s.} \quad (32)$$

and hence by virtue of (31), the convergence in (30) holds for all $z \in \overline{\mathcal{D}} \setminus \{-\alpha, \alpha\}$. Furthermore, (32), (31) and (26) imply that with probability one, uniformly on \mathcal{D}_δ for any $\delta > 0$,

$$\begin{aligned} \lim_{n \rightarrow \infty} \frac{1}{n} \log |U_n(z) - \varepsilon_x \alpha| &= \lim_{n \rightarrow \infty} \frac{1}{n} \log(1 - \varepsilon_x y_n) = - \lim_{n \rightarrow \infty} \frac{1}{n} \log(1 + \varepsilon_x \omega_n) \\ &= -\varepsilon_x \cdot \left(\lim_{n \rightarrow \infty} \frac{1}{n} \log \omega_n \right) = -|E(\gamma_1)|, \end{aligned} \quad (33)$$

where in the last step we used (10) and the ergodic theorem. \square

Recall G_α from (9). One can consider G_α as a topological group by equipping it with the topology of compact convergence on the complete metric space (\mathcal{D}, d_p) (which is the same as the topology of compact convergence on \mathcal{D} equipped with the usual planar topology). A natural compactification of G_α is obtained by adding to it two elements:

$$g_{+\infty} := q_{1,\alpha} = \frac{z + \alpha}{1 + \bar{\alpha}z} = \alpha \quad \text{and} \quad g_{-\infty} := q_{-1,\alpha} = \frac{z - \alpha}{1 - \bar{\alpha}z} = -\alpha. \quad (34)$$

Let \mathcal{K} and $\bar{\mathcal{K}}$ be, respectively, the sets of all compact (closed and bounded in the usual planar topology) subsets of \mathcal{D} and $\bar{\mathcal{D}}$, and

$$\mathcal{K}_\alpha := \{E \in \bar{\mathcal{K}} : \{-\alpha, \alpha\} \cap E = \emptyset\}$$

By definition, for any $x \in \mathbb{R}$ and a sequence of reals x_n , $n \in \mathbb{N}$,

$$\lim_{n \rightarrow \infty} g_{x_n} = g_x \quad \text{iff} \quad \forall E \in \mathcal{K}, \quad \lim_{n \rightarrow \infty} \sup_{z \in E} |g_{x_n}(z) - g_x(z)| = 0. \quad (35)$$

It is easy to check (see, for instance, (31) above) that

$$\lim_{n \rightarrow \infty} g_{x_n} = g_x \quad \text{iff} \quad \lim_{n \rightarrow \infty} x_n = x. \quad (36)$$

Thus the topology of G_α is inherited from \mathbb{R} . To justify the definitions in (34) observe that the equivalence in (36) still holds true for $x \in \{-\infty, +\infty\}$ if (35) is understood as the definition of the convergence in \bar{G}_α with \mathcal{K} replaced by \mathcal{K}_α .

Corollary 4.5. *Under the conditions of Theorem 4.3, $\lim_{n \rightarrow \infty} U_n = g_{+\infty \cdot \varepsilon_x}$ in the compact convergence topology induced by $\bar{\mathcal{D}} \setminus \{-\alpha, \alpha\}$.*

Recall circles H_z from (19) and bipolar coordinate $\tau(z)$ from (21). In view of Lemmas 3.1 and 3.4, assuming that $P(\gamma = 0) \neq 1$, we refer to the process $(U_n(z))_{n \in \mathbb{Z}_+}$ restricted to H_z as *oscillating at infinity* if with probability one,

$$\limsup_{n \rightarrow \infty} \tau(U_n(z)) = -\liminf_{n \rightarrow \infty} \tau(U_n(z)) = +\infty.$$

We call the process restricted to H_z *transient to infinity* if with probability one,

$$\text{either} \quad \lim_{n \rightarrow \infty} \tau(U_n(z)) = +\infty \quad \text{or} \quad \lim_{n \rightarrow \infty} \tau(U_n(z)) = -\infty.$$

The following proposition asserts a standard random walk dichotomy for $U_n(z)$. Namely, it implies that for all $z \in \mathcal{D} \setminus \{-\alpha, \alpha\}$, the process $U_n(z)$ is oscillating at infinity if and only if ω_n on \mathbb{R} is oscillating, and is transient to infinity otherwise.

Proposition 4.6. *Let Assumption 4.1 hold and assume in addition that $\varepsilon_x = 0$. Then for any $z \in \mathcal{D} \setminus \{-\alpha, \alpha\}$, the random walk $U_n(z)$ restricted to H_z is oscillating at infinity.*

Proof of Proposition 4.6. If Assumption 4.1 holds with $\varepsilon_x = 0$, then the (generalized) random walk ω_n is recurrent [2]. Thus the proposition is a direct implication of Lemma 3.1 combined together with the result of Lemma 3.4. \square

We next consider the following general assumption:

Assumption 4.7. *There exists a sequence of positive reals $(a_n)_{n \in \mathbb{N}}$ and a random variable W such that $\lim_{n \rightarrow \infty} a_n = +\infty$ and $\frac{\omega_n}{a_n}$ converges to W in distribution as $n \rightarrow \infty$.*

In the above assumption we do not exclude the case that W is degenerate. The most basic setup when Assumption 4.7 holds true is described by the classical central limit theorem. If $(x_n)_{n \in \mathbb{N}}$ is an i.i.d. sequence, $E(\gamma_1) = 0$ and $E(\gamma_1^2) \in (0, \infty)$, then W is a normal distribution and one can choose $a_n = \sqrt{n}$. The CLT holds in fact in a functional form and even in that form can be extended to martingales, functionals of Markov chains, mixing and other “weakly dependent in long range” sequences (see, for instance, [4, 17, 31] and references therein). The theorem can also be extended to sequences with infinite variance in the domain of attraction of a stable law W (see, for instance, [9] and references therein).

Let F_W denote the distribution function of W . It follows from (20) that

$$\frac{1}{a_n} \log \left| \frac{U_n(z) + \alpha}{U_n(z) - \alpha} \right| \Rightarrow W, \quad (37)$$

where \Rightarrow indicates the convergence in distribution. Our next result is a refinement of (37) that treats the numerator and denominator separately.

Theorem 4.8. *Let Assumption 4.7 hold. Then for any $z \in \overline{\mathcal{D}} \setminus \{-\alpha, \alpha\}$ and a real number $s > 0$ we have*

$$\lim_{n \rightarrow \infty} P\left(\frac{1}{a_n} \log |U_n(z) + \alpha| < -s\right) = F_W(-s) \quad (38)$$

and

$$\lim_{n \rightarrow \infty} P\left(\frac{1}{a_n} \log |U_n(z) - \alpha| < -s\right) = 1 - F_W(s). \quad (39)$$

The theorem is a counterpart of Theorem 4.3 under Assumption 4.7. We omit a formal proof of the theorem because it can be readily obtained through a suitable modification of the almost sure computation in (33). Indeed, (33) is in essence an observation that by virtue of (31) and (32), $|U_n(z) + \varepsilon \alpha|$ can only be small if $1 - \varepsilon y_n$ is small, in which case $|U_n(z) + \varepsilon \alpha| \sim c_z(1 - \varepsilon y_n)$ as $n \rightarrow \infty$, where $c_z > 0$ is a constant that depends on z . Here and henceforth the notation $u_n \sim v_n$ for two sequence of real numbers $(u_n)_{n \in \mathbb{N}}$ and $(v_n)_{n \in \mathbb{N}}$ stands for $\lim_{n \rightarrow \infty} \frac{u_n}{v_n} = 1$.

We note that in the generic situation when Assumption 4.7 holds true and W is distributed according to a stable law, the following limit exists:

$$\chi := \lim_{s \rightarrow \infty} \frac{1 - F_w(s)}{1 - F_W(s) + F_W(-s)} \in [0, 1].$$

In view of (38) and (39) this implies:

$$\lim_{s \rightarrow \infty} \lim_{n \rightarrow \infty} \frac{P(\log |U_n(z) + \alpha| < -sa_n)}{P(\log |U_n(z) - \alpha| < -sa_n)} = \frac{1 - \chi}{\chi}.$$

An important aspect of oscillations of one-dimensional random walks is captured by laws of iterated logarithm. For instance, we have

Proposition 4.9. *Suppose that x_n , $n \in \mathbb{N}$, form an i.i.d. sequence, $E(\gamma_1) = 0$, and $\sigma := (E(\gamma_1^2))^{1/2} \in (0, \infty)$. Then, for any $z \in \mathcal{D} \setminus \{-\alpha, \alpha\}$, with probability one,*

$$\limsup_{n \rightarrow \infty} \frac{B_\alpha(U_n(z))}{\phi(n)} = \limsup_{n \rightarrow \infty} \frac{B_{-\alpha}(U_n(z))}{\phi(n)} = \limsup_{n \rightarrow \infty} \frac{d_p(0, U_n(z))}{\phi(n)} = \sigma,$$

where $\phi(n) := \sqrt{2\pi n \log \log n}$.

We remark that the usual law iterated logarithm can be extended to sums of weakly dependent random variables (see, for instance, [7] and references therein) and (in a different form) to sequences with infinite variance [9]. Many interesting almost sure results about simple random walk can be found in [28].

5 A random walk on orthogonal pencils of circles

In this section we consider a random motion on $\overline{\mathcal{D}}$ which is intimately related to the evolution of the sequence $U_n(z)$ that we studied so far. The underlying idea is to adopt a pattern which is regular for the transition mechanism of random walks on \mathbb{Z}^2 and consider a discrete-time motion where two orthogonal coordinates changes in an alternating fashion, one at a time. The natural choice of the underlying coordinates within the context is the pair of bipolar coordinates (σ, τ) introduced in (21). We discuss here one, arguably the most simply related to $(U_n(z))_{n \in \mathbb{Z}_+}$ example of such a motion. Several other examples will be discussed by the authors elsewhere [27].

Before we proceed with the specific example, we recall that isoparametric curves in bipolar coordinates (i.e., curves along which only one coordinate in the pair (σ, τ) changes while another remains constant) constitute circles. More specifically, σ remains constant on circles H_z introduced in Lemma 3.1 (dashed circles in Fig. 3 below) whereas τ is constant on circles with centers lying on the line l_α , each one being orthogonal to every circle in the collection $(H_z)_{z \in \overline{\mathcal{D}}}$ (dotted circles in Fig. 3). In particular, circular arcs corresponding to constant τ are geodesic lines in the Poincaré disk model. The family of circles include two degenerate circles, namely the line l_α corresponding to $\sigma = \pi$ and an orthogonal to it which corresponds to $\tau = 0$. The family of coaxial circles corresponding to a constant σ are sometimes referred as to an elliptic pencil of (Apollonian [23]) circles. Similarly, the circles corresponding to a constant value of τ form a hyperbolic pencil [14, 21, 30]. The terminology is related to a representation of planar circles as projective lines in dimension 3.

Recall the bipolar coordinates (σ, τ) from (21). Rather than working directly with σ we will consider

$$\varsigma = \text{sign}(\sigma) \cdot \pi - \sigma, \quad \varsigma \in \left[-\frac{\pi}{2}, \frac{\pi}{2}\right].$$

This version of the angular component is a continuous function of the Cartesian coordinates. Furthermore,

$$\frac{z + \alpha}{\alpha - z} = e^{\tau(z) + i\varsigma(z)}, \quad \forall z \in \mathcal{D}.$$

We remark that similarly customized bipolar coordinates are used, for instance, in [29].

Fix any $p \in (0, 1)$ and let $q := 1 - p$. Let $(u_n)_{n \in \mathbb{N}}$ be a sequence of i.i.d. random variables, each one distributed uniformly over the interval $[-\frac{\pi}{2}, \frac{\pi}{2}]$. Let $(c_n)_{n \in \mathbb{Z}}$ be a sequence of Bernoulli random variables (“coins”) such that $P(c_n = 1) = p$ and $P(c_n = 0) = q$. Assume that the sequences $(x_n)_{n \in \mathbb{N}}$, $(u_n)_{n \in \mathbb{N}}$, and $(c_n)_{n \in \mathbb{N}}$ are independent each of other. Further, introduce the following auxiliary functionals of the sequence c_n : $S_n = \sum_{k=1}^n c_k$ and $k_n = \max\{t \leq n : c_t = 0\}$. We will consider the following random walk $(Z_n)_{n \in \mathbb{Z}_+}$ on the state space $\overline{\mathcal{D}}$. Let $Z_n = (\varsigma_n, \tau_n)_{\text{bipolar}}$ denote the location of the random walk at time $n \in \mathbb{Z}_+$ in the bipolar coordinates (ς, τ) . At each instant of time $n \in \mathbb{N}$, the random walk changes its location from Z_{n-1} to Z_n according to the following rule and independently of past events:

- If $c_n = 1$, then $Z_n = g_{\gamma_n}(Z_{n-1})$, thus $\varsigma_n = \varsigma_{n-1}$ and $\tau_n = \tau_{n-1} + \gamma_{S_n}$.
- If $c_n = 0$, then $\tau_n = \tau_{n-1}$ and $\varsigma_n = u_n$.

Thus Z_n is a Markov chain with transition kernel determined by

$$P(\varsigma_{n+1} \in A, \tau_{n+1} \in B \mid \varsigma_n, \tau_n) = p \cdot \mathbf{1}_{\{\varsigma_n \in A\}} \cdot P(g_{\gamma_1}(Z_{n-1}) \in B) + q \cdot \mathbf{1}_{\{\tau_n \in B\}} \cdot \frac{|A|}{\pi},$$

where $A \subset [-\frac{\pi}{2}, \frac{\pi}{2}]$ and $B \subset \mathbb{R}$ are Borel sets, $\mathbf{1}_E$ denotes the indicator function of a set E , and $|B|$ is the Lebesgue measure of the set B . Furthermore, for $n \in \mathbb{N}$,

$$(\varsigma_n, \tau_n) = c_n \cdot (\varsigma_{n-1}, \tau_{n-1} + \gamma_{S_n}) + (1 - c_n) \cdot (u_n, \tau_n)$$

and hence

$$(\varsigma_n, \tau_n) = (u_{k_n}, \tau_0 + \omega_{S_n}), \quad n \in \mathbb{N}.$$

In particular,

$$Z_n = U_{S_n}(\mathfrak{z}_n), \quad \text{where} \quad \mathfrak{z}_n := (\varsigma_n, \tau_n)_{\text{bipolar}} = (u_{k_n}, \tau_0 + \omega_{S_n})_{\text{bipolar}}. \quad (40)$$

The last formula allows to apply the results of the previous sections to the random walk Z_n . It turns out that even though, in contrast to $U_n(z)$, the distance $d_p(Z_n, 0)$ between Z_n and the origin can be arbitrarily large with a positive probability for any $n \in \mathbb{N}$ independently of the value of ω_n , the asymptotic behavior of the sequence Z_n is quite similar to that of U_n (see Theorems 5.2 and 5.4 and also Remark 5.3 below). In this sense, the former model of a random motion on $\overline{\mathcal{D}}$ seems to offer an adequate generalization of the latter.

Our main results in this section (Theorem 5.2 and Theorem 5.4 below) are not affected by the assumption on the position or distribution of the initial value σ_0 (basically, because $\varsigma_n = \varsigma_{k_n}$ would be anyway distributed uniformly over $[-\frac{\pi}{2}, \frac{\pi}{2}]$ for all n large enough, so that $k_n \geq 1$). For simplicity, we will assume throughout the rest of the paper that ς_n are distributed uniformly over $[-\frac{\pi}{2}, \frac{\pi}{2}]$ for all $n \in \mathbb{Z}_+$, namely:

Assumption 5.1. ς_0 is distributed uniformly over $[-\frac{\pi}{2}, \frac{\pi}{2}]$.

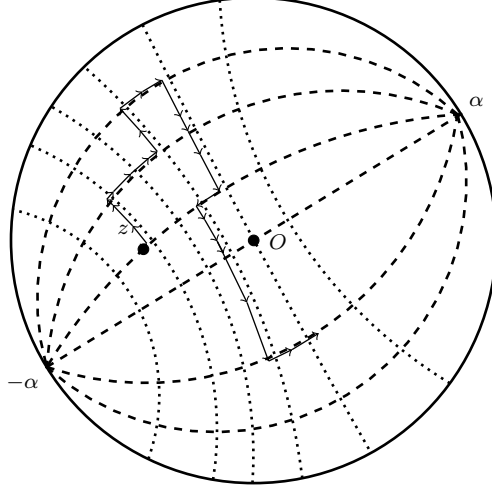


Figure 3: Random walk on orthogonal pencils of circles. Every dotted circle intersects every dashed circle at a right angle. Every dotted circle corresponds to some $\tau \in \mathbb{R}$ and every dashed circle corresponds to some $\varsigma \in [-\frac{\pi}{2}, \frac{\pi}{2}]$. The arrows indicate a random trajectory $\{U_n(z) : n = 0, \dots, 24\}$ obtained through numerical simulation.

We note that the randomness of S_n in (12) is a simple “removable” technicality since

$$Z_n = \frac{\mathfrak{z}_n + \alpha y_{S_n}}{1 + \bar{\alpha} y_{S_n} \mathfrak{z}_n} = \frac{\mathfrak{z}_n + \alpha \tilde{y}_n}{1 + \bar{\alpha} \tilde{y}_n \mathfrak{z}_n}, \quad (41)$$

where, similarly to (26),

$$\tilde{y}_n := y_{S_n} = \frac{e^{\tilde{\omega}_n} - 1}{e^{\tilde{\omega}_n} + 1} \quad \text{with} \quad \tilde{\omega}_n := \sum_{k=1}^n \gamma_k \cdot \mathbf{1}_{\{S_k = S_{k-1} + 1\}}, \quad (42)$$

and $\tilde{\gamma}_k := \gamma_k \cdot \mathbf{1}_{\{S_k = S_{k-1} + 1\}}$ are i.i.d. random variables. To illustrate the technicality arising from the randomness of \mathfrak{z}_n in (40) and (41) we will prove the following almost sure result, an analogue of Theorem 4.2 and Proposition 4.9 for the sequence Z_n .

Theorem 5.2. *Let $(Z_n)_{n \in \mathbb{Z}_+}$ be a random walk defined in (40). Then for any $\tau_0 \in \mathbb{R}$,*

(i) *Under Assumption 4.1, with probability one,*

$$\lim_{n \rightarrow \infty} \frac{1}{n} B_{\varepsilon_x \alpha}(Z_n) = -p \cdot |E(\gamma_1)| \quad \text{and} \quad \lim_{n \rightarrow \infty} \frac{1}{n} d_p(0, Z_n) = p \cdot |E(\gamma_1)|.$$

(ii) *Under the conditions of Proposition 4.9, with probability one,*

$$\limsup_{n \rightarrow \infty} \frac{B_\alpha(U_n(z))}{\phi(n)} = \limsup_{n \rightarrow \infty} \frac{B_{-\alpha}(U_n(z))}{\phi(n)} = \limsup_{n \rightarrow \infty} \frac{d_p(0, U_n(z))}{\phi(n)} = \sigma \sqrt{p},$$

where $\sigma = (E(\gamma_1^2))^{1/2} \in (0, \infty)$ and $\phi(n) := \sqrt{2\pi n \log \log n}$.

Proof of Theorem 5.2.

(i) The result will follow from (41) and (42) along with the results in Proposition 3.7 and Lemma 3.10 provided that we are able to show that the random initial condition doesn't interfere and destroy the almost sure convergence, namely that w. p. 1,

$$\lim_{n \rightarrow \infty} \frac{1}{n} B_{\varepsilon_x \alpha}(\mathfrak{z}_n) = \lim_{n \rightarrow \infty} \frac{1}{n} d_{\mathfrak{p}}(0, \mathfrak{z}_n) = 0. \quad (43)$$

Using the explicit formulas for the Poincaré distance and Buzemann functions, it is easy to check that (43) amounts to

$$\lim_{n \rightarrow \infty} \frac{1}{n} \log(1 - |\mathfrak{z}_n|) = 0 \quad \text{a. s.}$$

To facilitate the proof of the second part of the theorem we will show a more general

$$\lim_{n \rightarrow \infty} \frac{1}{n^\beta} \log(1 - |\mathfrak{z}_n|) = 0 \quad \text{a. s.} \quad (44)$$

for any $\beta > 0$. Toward this end observe that by virtue of (22) and (23), in the Cartesian coordinates we have

$$\mathfrak{z}_n \bar{\alpha} = i \cot\left(\frac{\varsigma_n}{2} + i \frac{\tau_0}{2}\right) = \frac{\sinh \tau_0}{\cosh \tau_0 + \cos \varsigma_n} \pm i \frac{\sin \varsigma_n}{\cosh \tau_0 + \cos \varsigma_n},$$

and hence

$$|\mathfrak{z}_n|^2 = \frac{\sin^2 \varsigma_n + \sinh^2 \tau_0}{(\cosh \tau_0 + \cos \varsigma_n)^2}.$$

Therefore,

$$1 - |\mathfrak{z}_n|^2 = \frac{2 \cos \varsigma_n}{\cosh \tau_0 + \cos \varsigma_n} \geq \frac{2 \cos \varsigma_n}{\cosh \tau_0 + 1}.$$

Thus, in order to prove (44) it suffices to show that, w. p. 1

$$\lim_{n \rightarrow \infty} \frac{1}{n^\beta} \log \cos \varsigma_n = 0,$$

or, equivalently,

$$P\left(\frac{1}{n^\beta} \log \cos \varsigma_n < -\varepsilon \text{ i. o.}\right) = 0, \quad \forall \varepsilon > 0.$$

By the Borel-Cantelli lemma, the last assertion is implied by the following one

$$\sum_{n=1}^{\infty} P((- \log \cos \varsigma_n)^{1/\beta} > \delta n), \quad \forall \delta > 0,$$

which in turn is equivalent to

$$E((- \log \cos \varsigma_n)^{1/\beta}) < \infty. \quad (45)$$

Let $s_n = \pi/2 - |\varsigma_n|$ and let $\bar{s} \in (0, \pi/2)$ be such that $\sin \bar{s} = \frac{\bar{s}}{2}$. Then $\sin s_n > \frac{\bar{s}}{2}$ for $s_n \in (0, \bar{s})$, and hence

$$E\left((- \log \cos \varsigma_n)^{1/\beta}\right) = E\left((- \log \sin s_n)^{1/\beta}\right) < \infty.$$

if $\int_0^{\bar{s}} (-\log s)^{1/\beta} ds < \infty$. Since the latter inequality holds true, so is (44). The proof of part (i) of the theorem is complete.

(ii) The proof of part (ii) is similar. Indeed, in view of (41) and (42) along with the results in Proposition 3.7 and Lemma 3.10 we only need to show that w. p. 1,

$$\lim_{n \rightarrow \infty} \frac{1}{\phi(n)} B_{-\varepsilon_x \alpha}(\mathfrak{z}_n) = \lim_{n \rightarrow \infty} \frac{1}{\phi(n)} d_{\mathfrak{p}}(0, \mathfrak{z}_n) = 0.$$

The latter identities follow from (44) with any $\beta < 1/2$. □

Remark 5.3. *We remark that the conclusions of Theorem 5.2 remains true for any distribution of i. i. d. random variables ς_n as long as the condition (45) is satisfied.*

Recall ε_x from (29). We conclude with a result showing that the assertions of Theorems 4.3 and 4.8 remain true for the sequence Z_n in place of $U_n(z)$. More specifically, we have the following:

Theorem 5.4.

(i) *Suppose that Assumption 4.1 is satisfied. If $\varepsilon_x \neq 0$, then*

$$\lim_{n \rightarrow \infty} \frac{1}{n} \log |Z_n - \varepsilon_x \alpha| = -p \cdot |E(\gamma_1)|, \quad \text{a. s.}$$

Moreover, the convergence is uniform on compact intervals in τ_0 .

(ii) *Let Assumption 4.7 hold. Then for all $\tau_0 \in \mathbb{R}$ and $s > 0$ we have*

$$\lim_{n \rightarrow \infty} P\left(\frac{1}{a_n} \log |Z_n + \alpha| < -s\right) = F_W(-s)$$

and

$$\lim_{n \rightarrow \infty} P\left(\frac{1}{a_n} \log |Z_n - \alpha| < -s\right) = 1 - F_W(s).$$

Proof of Theorem 5.4. Observe that for all $z \in \mathcal{D}$ and $\varepsilon \in \{-1, 1\}$, we have (see Fig. 3):

$$|U_n(z_-) - \varepsilon \alpha| \leq |U_n(z) - \varepsilon \alpha| \leq |U_n(z_+) - \varepsilon \alpha|, \quad (46)$$

where given $z = (\varsigma_0, \tau_0)_{\text{bipolar}}$, we define $z_- = (0, \tau_0)_{\text{bipolar}}$ and $z_+ = (\pi/2, \tau_0)_{\text{bipolar}}$. To verify claims (i) and (i) in the theorem, apply, respectively, Theorem 4.3 and Theorem 5.4, taking in account (40) and (42) along with (46). □

6 Numerical simulations of Z_n

This section contains results of the numerical simulation of the random walk Z_n introduced in Section 5. In all the scenarios reported below α is taken to be equal to 1, the number of steps is $n = 300,000$ and ς_0 is distributed uniformly over $[-\frac{\pi}{2}, \frac{\pi}{2}]$ with parameter p varying from case to case. Each figure below represents one random realization of the random walk with parameters as indicated above and further specified in the caption.

In Fig. 4, x_n is distributed uniformly over the interval $(-1, 1)$, and hence the underlying random motion is recurrent. When $p = 0.5$ most of the observations are located near the poles $\pm\alpha$. The more p deviates from 0.5, the more the cluster of observations appears to have a structure resembling a disjoint union of circles from one dominant pencil (dashed lines in Fig. 1 if p is close to one and dotted lines if p is close to zero).

In Fig. 5, x_n has a triangular density with mode 0.1 supported on $(-1, 1)$, namely in these three cases we have

$$P(x_n \in dx) = \begin{cases} \frac{100}{121}(x+1)dx & \text{if } -1 < x < \frac{21}{100}, \\ \frac{100}{79}(1-x)dx & \text{if } \frac{21}{100} < x < 1. \end{cases}$$

For this distribution, $\varepsilon_x = E(\gamma_1) \approx 0.0781$, and therefore the random walk is with probability one attracted to α by virtue of part (i) of Theorem 5.2 (since $\lim_{n \rightarrow \infty} B_\alpha(Z_n) = \infty$). It appears (see Fig. 5(c) below) that if p is large, then for an “intermediately large” number of steps n there is a “thick” cluster present around the repelling fixed point $\alpha = -1$. The explanation might be provided by (21) and Lemma 3.4, the fluctuations of U_n measured in the usual Euclidean distance are much large in magnitude near the poles $\pm\alpha$ than they are at points of the trajectory located far away from the boundary.

Acknowledgment

We would like to thank the anonymous referee for their very helpful comments and suggestions.

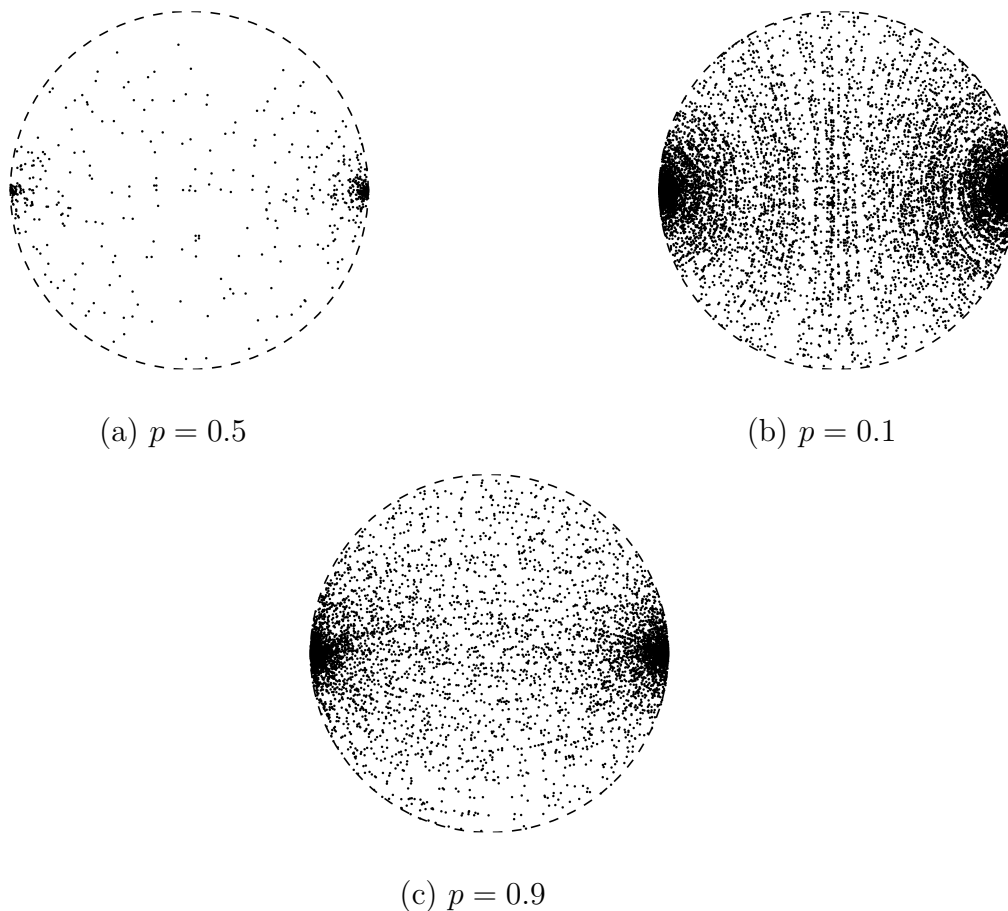


Figure 4: A realization of the random walk on Apollonian circles with $\alpha = 1$ (300,000 steps). Here we have x_n are i.i.d drawn from uniform distribution on $(-1, 1)$, and ς_0 is distributed uniformly over $[-\frac{\pi}{2}, \frac{\pi}{2}]$.

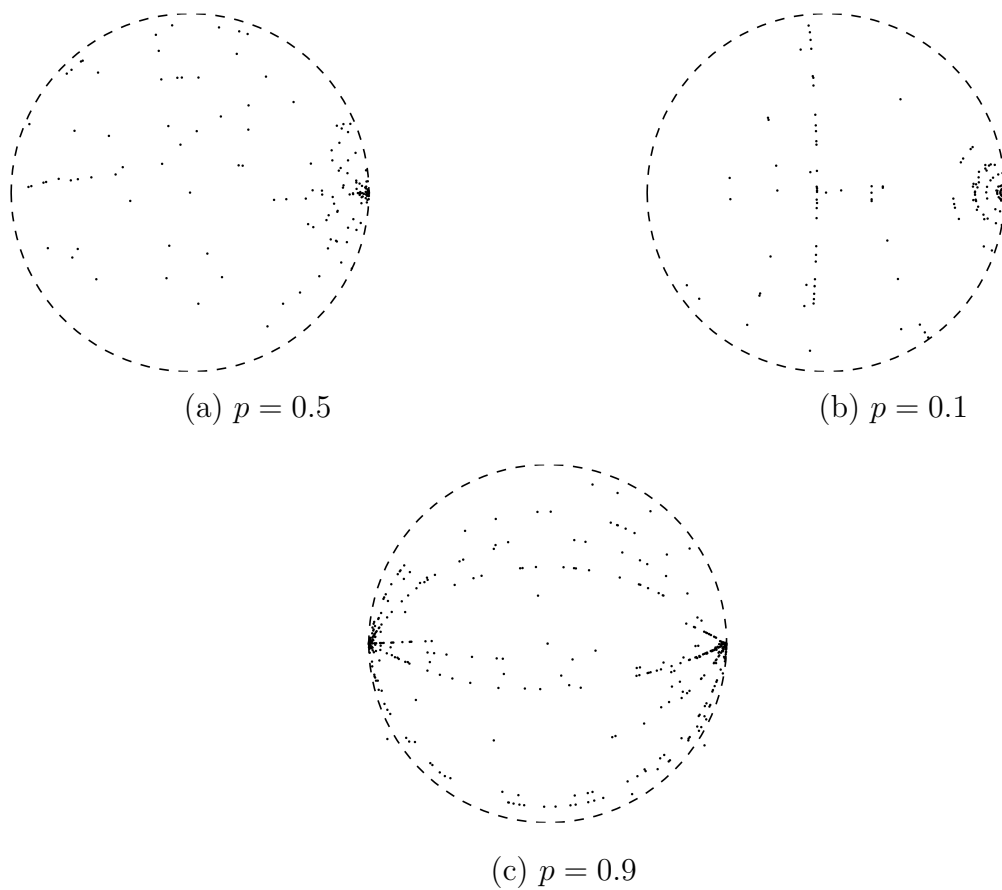


Figure 5: A realization of the random walk on Apollonian circles with $\alpha = 1$ (300,000 steps). Here x_n are i.i.d drawn from a triangular distribution on $(-1, 1)$ with mode 0.1, and ς_0 is distributed uniformly over $[-\frac{\pi}{2}, \frac{\pi}{2}]$.

References

- [1] A. Ambroladze and H. Wallin, *Random iteration of Möbius transformations and Furstenberg's theorem*, Ergodic Theory Dynam. Systems **20** (2000), 953–962.
- [2] G. Atkinson, *Recurrence of co-cycles and random walks*, J. London Math. Soc. **13** (1976), 486–488.
- [3] R. F. Bass, *Probabilistic Techniques in Analysis* (Springer Series in Probability and Its Applications), Springer, 1995.
- [4] B. Basrak, D. Krizmanić, and J. Segers, *A functional limit theorem for dependent sequences with infinite variance stable limits*, Ann. Probab. **40** (2012), 2008–2033.
- [5] H. Bateman, *Electrical and Optical Wave-Motion*, Dover 1955 (Reprint of 1914 Edition).
- [6] H. Bateman, *Spheroidal and bipolar coordinates*, Duke Math. J. **4** (1938), 39–50.
- [7] N. H. Bingham, *Variants on the law of the iterated logarithm*, Bull. London Math. Soc. **18** (1986), 433–467.
- [8] V. V. Borisov and A. B. Utkin, *Generalization of Brittingham's localized solutions to the wave equation*, Eur. Phys. J. B **21** (2001), 477–480.
- [9] A. A. Borovkov and K. A. Borovkov, *Asymptotic Analysis of Random Walks. Heavy-tailed Distributions*, Encyclopedia of Mathematics and its Applications Vol. 118, Cambridge University Press, 2008.
- [10] C. P. Boyer, E. G. Kalnins, and W. Miller, Jr., *Symmetry and separation of variables for the Helmholtz and Laplace equations*, Nagoya Math. J. **60** (1976), 35–80.
- [11] M. R. Bridson and A. Haefliger, *Metric spaces of non-positive curvature* (Fundamental Principles of Mathematical Sciences, Vol. 319), Springer-Verlag, Berlin, 1999.
- [12] S. Buyalo and V. Schroeder, *Elements of Asymptotic Geometry* (EMS Monographs in Mathematics), European Mathematical Society, 2007.
- [13] V. Cammarota and E. Orsingher, *Travelling randomly on the Poincaré half-plane with a Pythagorean compass*, J. Stat. Phys. **130** (2008), 455–482.
- [14] J. L. Coolidge, *A Treatise on the Circle and the Sphere*, Reprint of the 1916 edition. Chelsea Publishing Co., Bronx, N.Y., 1971.
- [15] J. Doob, *Classical Potential Theory and Its Probabilistic Counterpart*, (Springer Series Classics in Mathematics), Springer, 1st ed. 1984. Reprint 2001 edition.
- [16] J. Happel and H. Brenner, *Low Reynolds Number Hydrodynamics: With Special Applications to Particulate Media*, Mechanics of Fluids and Transport Processes Vol. 1, Springer, 1983.

- [17] G. L. Jones, *On the Markov chain central limit theorem*, Probab. Surv. **1** (2004), 299–320.
- [18] E. Jørgensen, *The central limit problem for geodesic random walks*, Z. Wahrscheinlichkeitstheorie und Verw. Gebiete **32** (1975), 1–64.
- [19] S. Karmakar and E. S. Key, *Compositions of random Möbius transformations*, Stoch. Analysis Appl. **22** (2004), 525–557.
- [20] S. Kato, *A Markov process for circular data*, J. R. Stat. Soc. Ser. B Stat. Methodol. **72** (2010), 655–672.
- [21] L. Keen and N. Lakic, *Hyperbolic Geometry from a Local Viewpoint* (London Mathematical Society, Student Text 68), Cambridge University Press, 2007.
- [22] M. Kelbert and Y. Suhov, *Large-time behavior of a branching diffusion on a hyperbolic space*, Theory Probab. Appl. **52** (2008), 594–613.
- [23] R. Klén and M. Vuorinen, *Apollonian circles and hyperbolic geometry*, J. Analysis **19** (2011), 41–60.
- [24] M. J. Morales, R. A. Diaz, and W. J. Herrera, *Solutions of Laplace’s equation with simple boundary conditions, and their applications for capacitors with multiple symmetries*, Journal of Electrostatics **78** (2015), 31–45.
- [25] E. Orsingher and A. De Gregorio, *Random motions at finite velocity in a non-Euclidean space*, Adv. in Appl. Probab. **39** (2007), 588–611.
- [26] M. A. Pinsky, *Isotropic transport process on a Riemannian manifold*, Trans. Amer. Math. Soc. **218** (1976), 353–360.
- [27] R. Rastegar and A. Roitershtein, *Random walks on confocal conics*, in preparation.
- [28] P. Révész, *Random Walk in Random and Non-Random Environments*, 3rd edn, World Scientific Publishing, Hackensack, NJ, 2013.
- [29] J. Sánchez-Reyes and L. Fernández-Jambrina, *Curves with rational chord-length parametrization*, Comput. Aided Geom. Design **25** (2008), 205–213.
- [30] H. Schwerdtfeger, *Geometry of Complex Numbers* (Dover Books on Mathematics) Revised ed., Dover Publications, 2012.
- [31] M. Tyran-Kamińska, *Convergence to Lévy stable processes under some weak dependence conditions*, Stoch. Proc. Appl. **120** (2010), 1629–1650.
- [32] A. A. Ungar, *The holomorphic automorphism group of the complex disk*, Aequat. Math. **47** (1994), 240–254.
- [33] A. A. Ungar, *Thomas precession: its underlying gyrogroup axioms and their use in hyperbolic geometry and relativistic physics*, Found. Phys. **27** (1997), 881–951.